Efficient Pipeline Guided-Wave Modeling via WFE Dispersion and Route-Based Propagation Including Spiral Paths

Ali Mardanshahi[1], Lotfollah Pahlavan[2], Mohammad Fotouhi[3], Koen Van Den Abeele[4], Dimitrios Chronopoulos[1]
[1]KU Leuven, Department of Mechanical Engineering & Mecha(tro)nic System Dynamics (LMSD), 9000, Belgium, ali.mardanshahi@kuleuven.be
[2]Department of Maritime and Transport Technology, Delft University of Technology, 2628CD, Delft, the Netherlands, l.pahlavan@tudelft.nl
[3]Department of Materials, Mechanics, Management and Design (3MD), Delft University of Technology, Mekelweg 5, 2628 CD Delft, Netherlands, m.fotouhi-1@tudelft.nl
[4]Wave Propagation and Signal Processing (WPSP), Department of Physics, KU Leuven – Campus Kula, Belgium, koen.vandenabeele@kuleuven.be

Abstract Reliable guided-wave monitoring of pipelines requires models that are both computationally efficient and capable of capturing the main physical propagation mechanisms in cylindrical waveguides. In thin-walled large-diameter pipes, guided waves propagate locally in a plate-like manner while the cylindrical topology creates multiple deterministic surface-geodesic routes between actuator and sensor locations. Besides the direct route, spiral routes wrapping around the circumference can generate distinct received wave packets, and additional packets arise from reflections at pipe boundaries and local discontinuities. This paper presents a semi-analytical hybrid framework for pipeline guided waves that combines Wave Finite Element (WFE) dispersion extraction with a route-based long-range propagation engine. The model explicitly accounts for direct and spiral propagation routes as well as boundary-reflected contributions. Validation is performed in two steps. First, model predictions are compared to full 3D transient finite element simulations on a steel pipe, assessing arrival times, wave-packet structure, and route-dependent contributions. Second, experimental measurements on a steel pipe are used to identify and interpret the received wave packets. The results demonstrate that the proposed semi-analytical model captures the dominant wave packets observed in 3D FE and experiments, while requiring significantly lower computational effort than full transient simulation. The validated framework provides a foundation for subsequent model-assisted monitoring and data-driven localization studies in realistic pipeline environments.

Keywords: Ultrasonic guided waves; Pipelines; Wave Finite Element (WFE); Route-based propagation; Spiral paths

https://doi.org/10.58286/33808

1. Introduction

Ultrasonic guided waves can propagate over long distances with relatively low attenuation, which makes them highly attractive for the inspection and monitoring of pipeline systems from a limited number of transducer locations [1, 2]. For pipeline applications, practical monitoring must cope with dispersive multimodal propagation, and with geometric features such as welds, joints, clamps, diameter transitions, and bends, which introduce reflection, transmission, and mode conversion [3, 4]. As a result, accurate and computationally efficient forward models are essential for reliable model-based analysis of guided-wave measurements.

Although full finite element (FE) simulations can model guided-wave propagation and scattering with high accuracy, they are computationally expensive because they require fine spatial and temporal discretization, especially for long-range problems with multiple structural features [5, 4]. To reduce this burden, several semi-analytical and reduced-order approaches have been developed. The semi-analytical finite element (SAFE) method combines an exponential representation in the propagation direction with FE discretization over the cross-section or thickness [6]. Other efficient alternatives include the Combined Analytical FE Model (CAFA) and the Scaled Boundary Finite Element Method (SBFEM), both applied to guided-wave modeling in isotropic structures [7]. Another important approach is the Wave Finite Element (WFE) method, which combines FE analysis with wave theory and computes wave characteristics from only a periodic segment, making the cost largely independent of the total waveguide length [8]. WFE has been widely used for structural identification, damage detection, multi-scale wave propagation, transient UGW simulations, and scattering analysis [9, 10]. In addition, ray-based or modal-ray methods provide a low-cost option for long-range propagation once the modal properties are known [11].

For structures with localized discontinuities, an efficient strategy is to separate the problem into propagation in uniform sections and scattering at structural features. In such a framework, WFE can describe wave propagation in the regular pipe segments, while reflection and transmission characteristics at welds or joints can be obtained from local numerical models in the form of scattering information [8]. These ingredients can then be coupled with ray-based or other high-frequency propagation schemes to simulate long-range wave motion without performing a full transient analysis of the entire pipeline [4]. Such hybrid strategies are especially appealing for inverse problems and monitoring applications, where repeated simulations are often required.

This paper proposes a semi-analytical guided-wave model for pipelines that combines WFE-based dispersion characterization with a route-based long-range propagation engine. The model assembles the received response by accounting for direct ($n = 0$), spiral wrap-around ($n = \pm 1$), and end-reflected wave packets, enabling physically interpretable identification of measured arrivals without full 3D transient simulation of the entire structure. The remainder of the paper is structured as follows. Section 2 introduces the hybrid modeling framework, including WFE-based dispersion extraction and route-based propagation with spiral and boundary-reflected sequences. Section 3 summarizes the 3D FE reference model and comparison protocol, while Section 4 describes the experimental setup and the identification of direct, spiral, and boundary-reflected wave packets in measurements. Finally, Section 5 concludes key findings, limitations, and outlook for model-assisted guided-wave interpretation in pipelines.

2. Background: Hybrid WFE–Ray Modeling Framework

2.1 WFE dispersion extraction for pipeline sections

Wave Finite Element (WFE) computes guided-wave dispersion in waveguides by enforcing phase-shift (Bloch/Floquet) relations between degrees of freedom on opposite boundaries of a representative segment [12, 13]. For a uniform pipeline section (or a locally plate-like pipe wall), WFE provides: (i) dispersion curves $k_m(\omega)$, (ii) associated mode shapes, and (iii) energy/flux quantities used for consistent modal normalization.

In practice, a small rectangular segment in the (x, y) plane is modeled and meshed through the thickness, with nodes arranged identically on opposite faces (Fig. 1). Under time-harmonic motion at frequency ω, the segment is described by a dynamic stiffness matrix $\mathbf{D}(\omega) = \mathbf{K} + i\omega\mathbf{C} - \omega^2\mathbf{M}$. Enforcing periodicity leads to an eigenproblem whose solutions provide the propagation constants (equivalently wavenumbers) and the corresponding modal displacement/force fields. The approach is applicable beyond isotropic plates, including multilayered structures that are homogeneous in-plane and vary through thickness [14, 15].

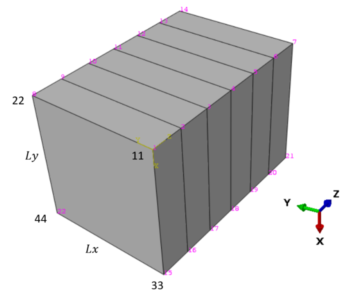

Fig. 1. *Representative 3D segment used for WFE dispersion extraction (schematic/ABAQUS model).*

2.2 Local feature characterization via scattering matrices

Localized features such as welds, joints, or thickness transitions can be treated as discontinuities connecting two uniform sections. In the frequency domain, their effect on guided waves is conveniently represented by a *scattering matrix* that maps incident modal amplitudes to reflected and transmitted amplitudes [11]. For a two-sided feature,

$$\begin{bmatrix} \mathbf{a}_{\mathrm{L}}^{-} \\ \mathbf{a}_{\mathrm{R}}^{+} \end{bmatrix} = \mathbf{S}(\omega) \begin{bmatrix} \mathbf{a}_{\mathrm{L}}^{+} \\ \mathbf{a}_{\mathrm{R}}^{-} \end{bmatrix}, \tag{1}$$

where $\mathbf{a}^+$ and $\mathbf{a}^-$ denote incident and outgoing (reflected or transmitted) modal amplitude vectors, respectively. In this work, $\mathbf{S}(\omega)$ is obtained by coupling WFE modal bases to a local FE or FE/WFE model of the feature (details depend on feature geometry). A common benchmark is a butt joint configuration (Fig. 2), for which the scattering matrix compactly captures reflection and transmission, including mode conversion, across the interface [14].

2.3 Ray-based (pencil) long-range propagation and assembly

Given dispersion data $k_m(\omega)$ and (when present) feature scattering matrices $\mathbf{S}(\omega)$, long-range propagation is assembled by propagating modal contributions between interaction points (source, features, boundaries, sensors). For a mode m traveling over distance L, the frequency-domain propagation factor is

$$H_m(\omega; L) = \exp(-ik_m(\omega)\, L)\, \exp(-\alpha_m(\omega) L)\,, \tag{2}$$

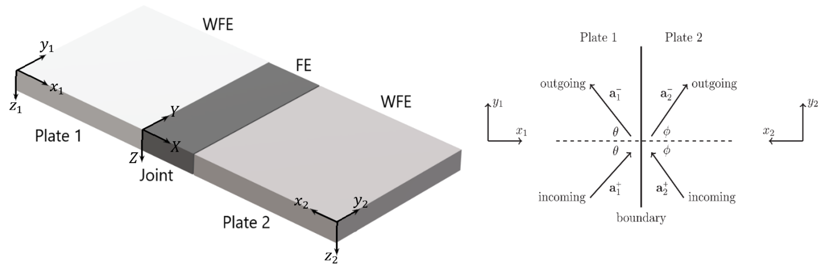

Fig. 2. *Two plate sections connected by a finite joint region (benchmark configuration). Reprinted and modified from [14].*

where $\alpha_m(\omega)$ is an optional effective attenuation coefficient. Multiple reflections/transmissions are included by enumerating the dominant interaction sequences and summing their contributions; in practice, the sequence set is truncated based on diminishing amplitude.

To model amplitude evolution and boundary reflections efficiently, we adopt a modal *guided-wave pencil* concept [16]. A pencil is a bundle of paraxial rays that infinitesimally diverge from an axial ray representing a specific energy direction, as illustrated in Fig. 3. The pencil formulation captures geometrical spreading and reflection-induced focusing/defocusing with minimal computational cost, while using WFE-derived dispersion to represent dispersive phase accumulation.

For the present scope, the pencil concept is used primarily to (i) propagate dominant wave packets over long distances and (ii) account for end-boundary reflections in a structured way. The total response at an observation point is then obtained by summing the contributions of the selected modal routes/sequences, yielding a fast semi-analytical predictor suitable for interpreting distinct received wave packets.

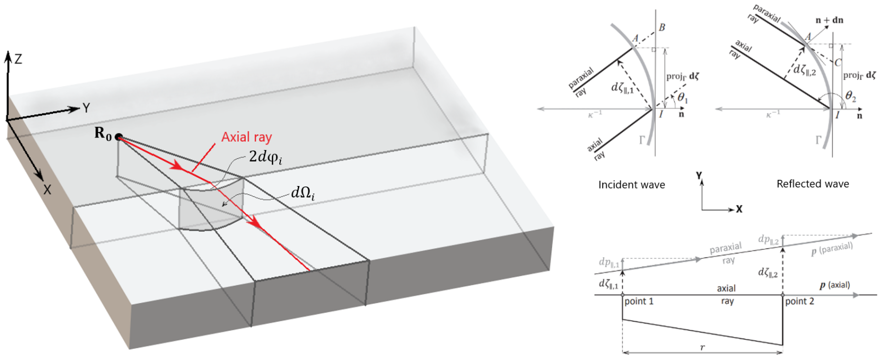

Fig. 3. *Schematic guided-wave pencil: an axial ray with infinitesimally close paraxial rays used to represent amplitude evolution and boundary reflections. Reprinted and modified from [16].*

2.4 Point-source assumption and finite-aperture extension.

The semi-analytical hybrid method is intended for long-range propagation in large, plate-like structures, where the source footprint is small compared to both propagation distances and the wavelengths of interest. In this regime, modelling the excitation as a *point source* is appropriate and consistent with practical devices such as dry-point contact (DPC) transducers.

Limitations. For short stand-off distances (near field) or for bonded patches whose lateral size is not negligible relative to the wavelength, a point-source model may bias amplitudes/directivity and introduce phase errors. In such cases, near-field interpretations should be avoided or a finite-aperture representation should be adopted.

Finite-size (aperture) source model. Following [16], a finite transducer is modelled by integrating (numerically summing) modal phase and amplitude contributions over the transducer footprint. The footprint is discretized into a set of source points; for each modal sequence, contributions from all points to the observation location are computed and summed. This spatial convolution captures finite-aperture effects while preserving the efficiency of the semi-analytical formulation, and naturally reduces to the point-source limit at long range.

2.5 Extension to cylindrical pipelines: direct and spiral routes

In large-diameter, thin-walled cylindrical pipes, guided-wave behavior can be treated as locally plate-like while the global topology introduces circumferential periodicity. We map the cylindrical surface to an unwrapped domain (z, s) with

$$s = R\theta, \tag{3}$$

and circumference

$$C = 2\pi R. \tag{4}$$

For a source at (z_a, s_a) and receiver at (z_r, s_r), define

$$\Delta z = z_r - z_a, \qquad \Delta s_0 = s_r - s_a, \tag{5}$$

with Δs_0 mapped to $(-C/2, C/2]$. The receiver admits image points at $s_r + nC$ with wrap index $n \in Z$, leading to multiple surface-geodesic routes of length

$$L_n = \sqrt{(\Delta z)^2 + (\Delta s_0 + nC)^2}. \tag{6}$$

The direct path corresponds to $n = 0$, while $n = \pm 1$ represent spiral routes wrapping once around the circumference in opposite directions. Within the proposed hybrid framework, each admissible route is treated as a propagation segment whose length is L_n, while the modal dispersion and feature scattering information are provided by the WFE/FE-WFE stages. This enables modeling of multiple deterministic arrivals in cylindrical measurements (direct and spiral) with minimal additional computational cost.

2.6 The proposed methodology

A Matlab/Python code has been developed alongside ABAQUS to merge the modal pencil method with WFE and FE/WFE techniques for efficient guided-wave simulation in finite structures. The process starts by capturing the applied point-load (or actuator) signal and computing its FFT. For each frequency line, WFE provides wave characteristics and energy flux quantities, ray tracing determines the paths (modal sequences) through boundaries and interfaces, and FE/WFE provides reflection/transmission coefficients and mode conversions at features. The propagation matrices and Green's functions are then assembled for each sequence and summed to obtain the frequency-domain displacement field, which is transformed back to time domain by inverse FFT. For cylindrical pipelines, propagation distances in each sequence are replaced by the route lengths L_n in Eq. (6), accounting for direct and spiral routes.

Figure 4 summarizes the proposed workflow. WFE is used to compute dispersion relations and modal quantities for the pipeline wall, while local FE/WFE models can provide scattering information at features when needed. A route-based propagation engine then assembles the sensor response by combining direct, spiral, and end-reflected sequences in the time/frequency domain.

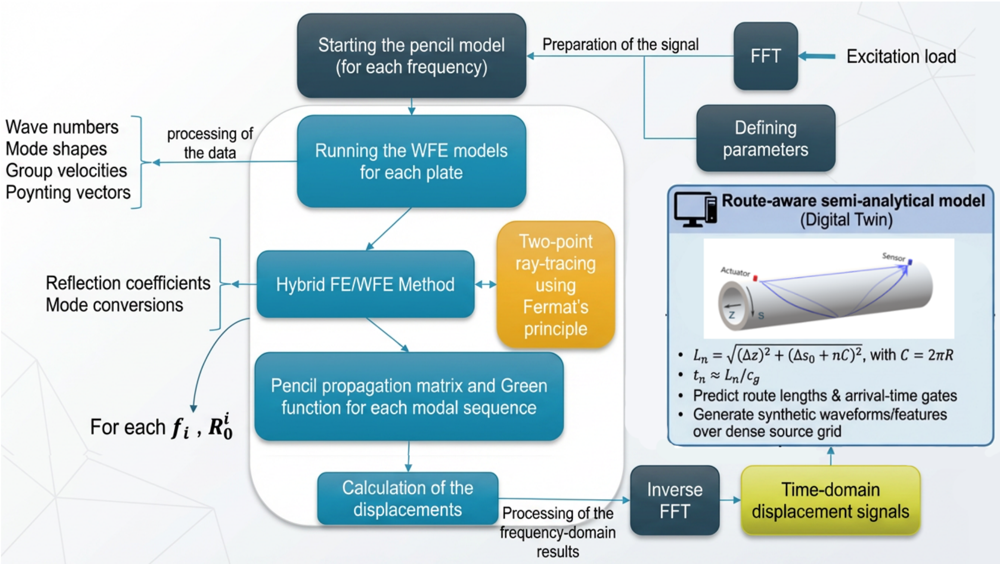

Fig. 4. *Proposed workflow: WFE-based dispersion extraction, optional local feature scattering characterization, and route-based long-range propagation including direct, spiral, and end-reflected sequences.*

3. 3D Finite Element Validation

3.1 3D transient FE model

Validation of the numerical case study is performed against full 3D FE dynamic/explicit simulations in ABAQUS with the exact geometries and material properties. The models use linear C3D8 elements with a maximum element size of 1 mm, satisfying the CFL stability requirement and providing at least eight nodes per wavelength for the relevant $A0$ and $S0$ modes across the operating bands, and the tone burst excitation with a centre frequency $f_c = 100$ kHz.

To suppress spurious boundary reflections, absorbing layers by increasing damping (ALID) are applied on three sides, following [17]. Rayleigh damping is used,

$$\mathbf{C} = \alpha\,\mathbf{M} + \beta\,\mathbf{K},$$

and only the mass-proportional term is activated in the absorbing region ($\beta = 0$). The damping is smoothly ramped through the layer thickness,

$$\alpha(x) = \alpha_M \left(\frac{x}{L}\right)^p, \qquad p = 2, \quad x \in [0, L],$$

with $L = 0.5$ m and $\alpha_M = 2\pi f_c$. The layer is discretized into four sublayers with increasing α. This ALID configuration maintains a stable explicit time step (diagonal mass), effectively absorbs outgoing waves, and avoids the need for domain enlargement, enabling a clean comparison with the SAHM predictions. As shown in Fig. 5, the 3D transient FE model includes the actuator and sensor locations on the steel pipe and an absorbing region to suppress end reflections.

3.2 FE validation results

Figure 6 compares the semi-analytical prediction with the 3D FE response at a representative sensor. The main wave packets are consistently reproduced: the earliest arrival corresponds to the direct route ($n = 0$), followed by later spiral packets ($n = \pm1, \pm2$) and the same for

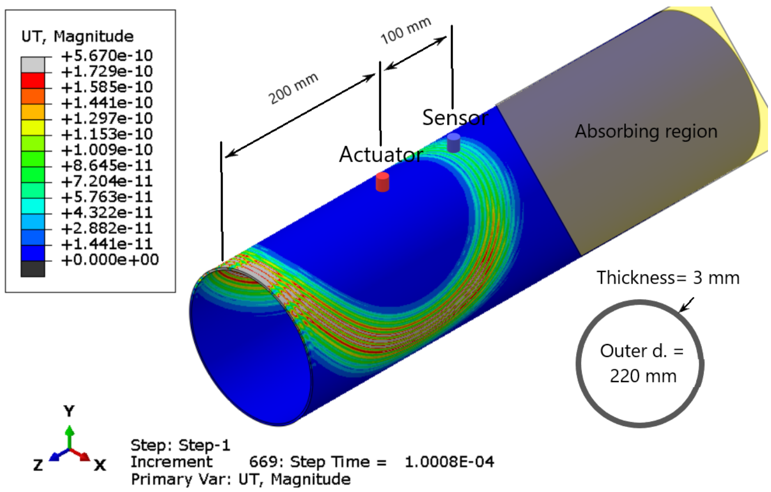

Fig. 5. *3D transient FE model of the steel pipe, indicating the actuator/sensor placement and the absorbing region.*

the end-reflected contribution. Overall, the semi-analytical model captures the packet ordering and relative timing well, while small differences in amplitude and fine oscillatory content are expected due to sensor/actuator idealizations and attenuation or boundary-condition mismatches in the FE reference.

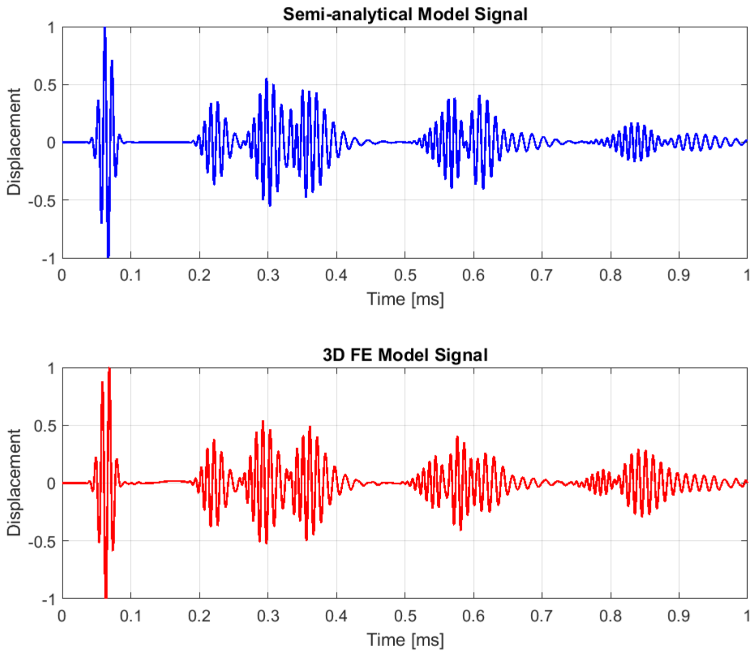

Fig. 6. *FE vs semi-analytical responses at a representative sensor, for the direct ($n = 0$), spiral ($n = \pm 1$ and $n = \pm 2$), and end-reflected packets.*

4. Experimental Validation on a Steel Pipe

4.1 Experimental setup and acquisition

Experiments are conducted on a 2 m steel pipe instrumented with an actuator and multiple sensors. A toneburst excitation with a centre frequency of about $f_c = 130$ kHz is applied due to the available transducer bandwidth, and responses are recorded at multiple sensor locations via a 4-channel acoustic emission system by SHM NEXT, and data processing system to observe propagating wave packets. Figure 7 shows the experimental setup. The acquisition settings (sampling rate, record length, averaging) are selected to resolve the targeted wave packets and capture end reflections.

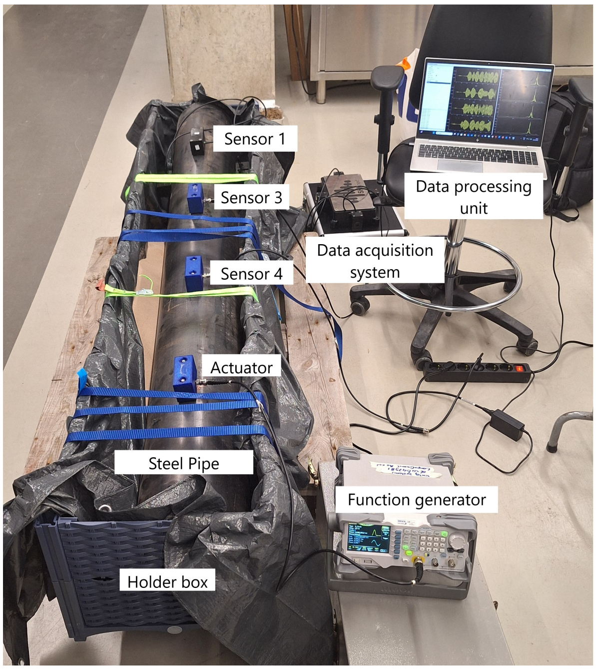

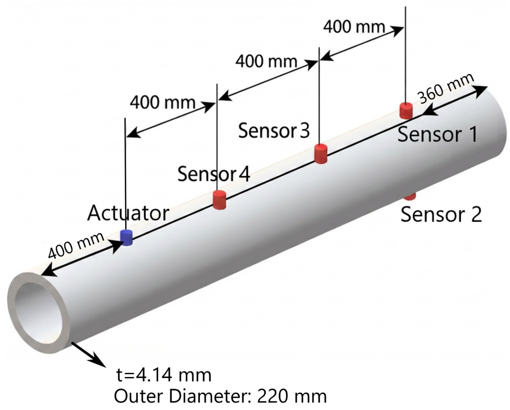

Fig. 7. *Experimental setup (steel pipe instrumentation).*

4.2 Wave-packet identification in measurements

Measured signals are filtered around the excitation band and compared with the model prediction to aid wave-packet identification. Arrival windows predicted by the semi-analytical model are overlaid on measured traces to associate observed packets with (i) direct routes, (ii) spiral routes, and (iii) boundary reflections. Figure 8 compares measured responses (S1–S4) with the corresponding semi-analytical predictions. The model correctly reproduces the main wave-packet structure and arrival ordering across sensors, allowing direct, spiral, and end-reflected packets to be identified using the predicted arrival windows. Small discrepancies in amplitude and late-time content are attributed to experimental factors (location and coupling variability, and sensor response).

The validation study targets the core physical mechanisms relevant to pipeline guided-wave interpretation: direct routes, spiral wrap-around routes, and end-boundary reflections. Agreement with 3D transient FE provides confidence that the semi-analytical model captures the dominant propagation physics while offering substantially lower computational cost. Wave-packet identification in the experimental measurements further supports practical relevance and indicates that spiral packets are observable and interpretable in real signals rather than being treated as unstructured artifacts.

Remaining challenges include robust amplitude prediction (sensitive to transducer coupling and material damping), more detailed modeling of complex weld/joint geometries, and systematic treatment of uncertainty in boundary reflection coefficients. Ongoing work extends the validated framework toward model-assisted monitoring tasks (e.g., calibration, localization, and data-driven fusion), while preserving the validated route-based interpretation.

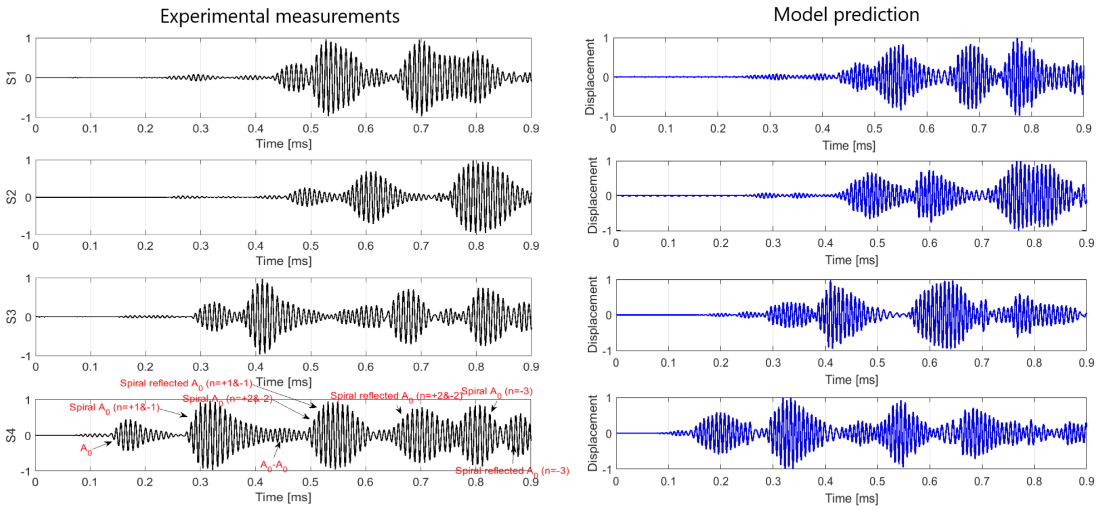

Fig. 8. *Experimental (left) and semi-analytical (right) sensor responses (S1–S4), showing direct, spiral, and end-reflected wave packets based on the model-predicted arrival windows.*

5. Conclusion

This paper presented a feasibility study of a semi-analytical guided-wave modeling framework for pipelines. The model combines WFE-derived dispersion with a route-based propagation engine that explicitly accounts for direct and spiral routes as well as boundary-reflected sequences. Validation is performed against full 3D transient finite element simulations. The validated model is utilized as the baseline for the experimental measurements on a steel pipe, with emphasis on identifying distinct received wave packets corresponding to direct, spiral, and end-reflected propagation. The results provide a structured baseline for subsequent model-assisted monitoring and data-driven localization studies in pipeline environments.

Acknowledgments

This work was supported by the Research Foundation – Flanders (FWO), Belgium, under FWO file ID V420825N. The authors would like to acknowledge SHM Next, Delft, for their valuable support in this research.

References

[1] Joseph L. Rose. An introduction to ultrasonic guided waves. Tutorial presented at MENDT 2007, 2007. Available via NDT.net.

[2] Joseph L. Rose. *Ultrasonic Guided Waves in Solid Media*. Cambridge University Press, Cambridge, UK, 2014.

[3] Peter Cawley. Long range inspection of structures using low frequency guided waves. *Structural Health Monitoring*, 2(2):137–154, 2003.

[4] A. M. Qadri, P. Huthwaite, M. J. S. Lowe, and T. K. Vogt. Assessing accuracy of an efficient analytical-finite element framework for modelling guided wave scattering from corrosion defects in pipes. *NDT & E International*, 156:103471, 2025.

[5] Muhammad Khalid Malik, Dimitrios Chronopoulos, and Gregor Tanner. Transient ultrasonic guided wave simulation in layered composite structures using a hybrid wave and finite element scheme. *Compos. Struct.*, 246:112376, 2020.

[6] Z A B Ahmad, J M Vivar-Perez, and Ulrich Gabbert. Semi-analytical finite element method for modeling of lamb wave propagation. *CEAS Aeronaut. J.*, 4(1):21–33, 2013.

[7] Hauke Gravenkamp, Carolin Birk, and Chongmin Song. Simulation of elastic guided waves interacting with defects in arbitrarily long structures using the scaled boundary finite element method. *J. Comput. Phys.*, 295:438–455, 2015.

[8] N. Aimakov, G. Tanner, and D. Chronopoulos. A wave finite element approach for modelling wave transmission through laminated plate junctions. *Scientific Reports*, 12:1852, 2022.

[9] Dimitrios Chronopoulos, C Droz, R Apalowo, M Ichchou, and W J Yan. Accurate structural identification for layered composite structures, through a wave and finite element scheme. *Compos. Struct.*, 182:566–578, 2017.

[10] Ali Mardanshahi, Koen Van Den Abeele, and Dimitrios Chronopoulos. Semi-analytical hybrid modeling of wave propagation for high-efficiency ultrasound inspection in large plate-like structures. *Smart Materials and Structures*, 34(11):115035, nov 2025.

[11] Emanuele Manconi and Brian R. Mace. Estimation of scattering matrices from wave finite element models and their application to waveguides. *Journal of Sound and Vibration*, 330(18–19):4643–4663, 2011.

[12] Brian R. Mace and Emanuele Manconi. Modelling wave propagation in two-dimensional structures using finite element analysis. *Journal of Sound and Vibration*, 318(4–5):884–902, 2008.

[13] Emanuele Manconi and Brian R. Mace. Wave characterisation of structural waveguides by means of the wave finite element method. *Journal of Sound and Vibration*, 332(7):1704–1716, 2009.

[14] Giannoula Mitrou, Neil Ferguson, and Jamil Renno. Wave transmission through two-dimensional structures by the hybrid FE/WFE approach. *Journal of Sound and Vibration*, 389:484–501, 2017.

[15] Jamil M Renno and Brian R Mace. Calculating the forced response of two-dimensional homogeneous media using the wave and finite element method. *Journal of sound and vibration*, 330(24):5913–5927, 2011.

[16] Jordan Barras, Alain Lhémery, and Alexandre Impériale. Modal pencil method for the radiation of guided wave fields in finite isotropic plates validated by a transient spectral finite element method. *Ultrasonics*, 103(January):106078, 2020.

[17] Alexander Velichko and Paul D. Wilcox. A generalized approach for efficient finite element modeling of elastodynamic scattering in two and three dimensions. *J. Acoust. Soc. Am.*, 128(3):1004, 2010.